HAL
open science

Configurationally stable dithia[7]helicene and dithia-quasi[8]circulene fused dithiolones

Maxime Baudillon, Thomas Cauchy, Nicolas Vanthuyne, Narcis Avarvari, Flavia Pop

To cite this version:

Maxime Baudillon, Thomas Cauchy, Nicolas Vanthuyne, Narcis Avarvari, Flavia Pop. Configurationally stable dithia[7]helicene and dithia-quasi[8]circulene fused dithiolones. Organic Chemistry Frontiers, 2022, 9 (16), pp.4260-4270. 10.1039/D2QO00921H . hal-03781234v2

HAL Id: hal-03781234

https://univ-angers.hal.science/hal-03781234v2

Submitted on 14 Mar 2023

HAL is a multi-disciplinary open access archive for the deposit and dissemination of scientific research documents, whether they are published or not. The documents may come from teaching and research institutions in France or abroad, or from public or private research centers.

L'archive ouverte pluridisciplinaire **HAL**, est destinée au dépôt et à la diffusion de documents scientifiques de niveau recherche, publiés ou non, émanant des établissements d'enseignement et de recherche français ou étrangers, des laboratoires publics ou privés.

Distributed under a Creative Commons Attribution - NonCommercial - NoDerivatives 4.0 International License

Configurationally stable dithia[7]helicene and dithia-quasi[8]circulene fused dithiolones†

Maxime Baudillon,[a] Thomas Cauchy,[a] Nicolas Vanthuyne,[b] Narcis Avarvari*[a] and Flavia Pop*[a]

Dithia-[7]helicene and quasi[8]circulene have been formed on the 1,3-dithiol-2-one ring by oxidative dehydrocyclisation of bis-naphthothiophenyl-1,3-dithiol-2-one. Quasi-circulenes are easily obtained at room temperature by successive dehydrocyclisations regardless the amount of oxidation reagent whereas selectivity towards helicene, involving a single dehydrocyclisation, has been achieved only at low temperature. DFT calculations suggest a mechanism *via* a dication intermediate rather than a mono-cation for the formation of the quasi-circulenes whereas the helicene should be formed *via* a radical cation intermediate. While dithia[7]helicene is known to give stable stereoisomers, here the unsubstituted dithia-quasi[8]circulene shows unprecedented configurational stability of the enantiomers, with a theoretically estimated enantiomerisation energy barrier of 30.4 kcal mol^{-1}, in excellent agreement with the experimentally determined value of 29.8 kcal mol^{-1}. The enantiomers of both helicene and quasi-circulene have been separated by chiral chromatography and their absolute configuration assigned from the calculated CD spectra.

1. Introduction

[*n*]Helicenes are aromatic compounds with inherent chirality built of *n ortho*-fused aromatic rings along a helical axis. They have long been known for their high specific optical rotation, strong absorption and emission of circularly polarized luminescence and have been recently intensively used for molecular recognition and chiral induction, as chiroptical switches or found applications in catalysis, chiral photonics and spintronics.[1–3] Their chiroptical properties arise from the inherent chirality coupled with the nonplanar π-delocalization on the whole polycyclic aromatic system. The introduction of heteroatoms into the fused helical polycyclic system, providing hetero-helicenes, offers new synthetic opportunities together with the possibility to tune their electronic and optoelectronic properties.[4] Similarly to [*n*]helicenes, [*n*]circulenes are formed of *n ortho*-fused rings except they have a cyclic disposition around a central ring with *n* sides. Removal of a CH═CH vinylene unit from one ring of the parent [*n*]circulenes (as highlighted in Chart 1) gives quasi[*n*]circulenes. Such cyclic structures are formed when the terminal positions of the helicene are connected by a σ bond, and have been used in the synthetic pathway of circulenes. Wynberg *et al.*[5] have referred them as "dehydrohelicenes" because they were obtained by dehydrogenation of the corresponding [*n*]helicenes through a Scholl reaction (in the presence of Friedel-Craft catalysts), their results indicating a limitation of the dehydrogenation reaction to hetero-[5] and -[6]helicenes. Recently, Itami *et al.*[6,7] and Wu *et al.*[8] have shown that quasi-circulenes can be formed from [6] and [7]helicenes, respectively. This family of polycyclic aromatic systems represents an emerging and unexplored class of materials with structures similar to either helicenes or circulenes. Depending on their composition and substitution scheme they can adopt flat, twisted or saddle-like topologies.[9] As shown by Rajca *et al.*,[10] heptathia[8]circulenes have flat geometry whereas an increasing number of phenyl rings in the helix structure of hetero-quasi[8]circulenes induces a proportional distortion of the geometry (Fig. S1, ESI†).

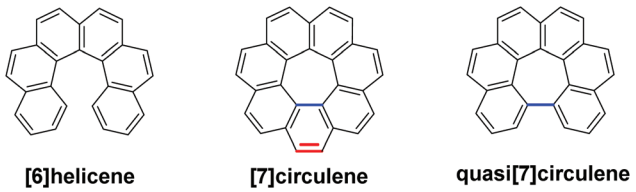

Chart 1 Structures of carbo-[6]helicene, [7]circulene and quasi[7]circulene.

[a]*Univ Angers, CNRS, MOLTECH-Anjou, SFR MATRIX, F-49000 Angers, France. E-mail: narcis.avarvari@univ-angers.fr, flavia.pop@univ-angers.fr*

[b]*Aix Marseille Université, CNRS, Centrale Marseille, iSm2, Marseille, France*

CCDC 2160878–2160881.

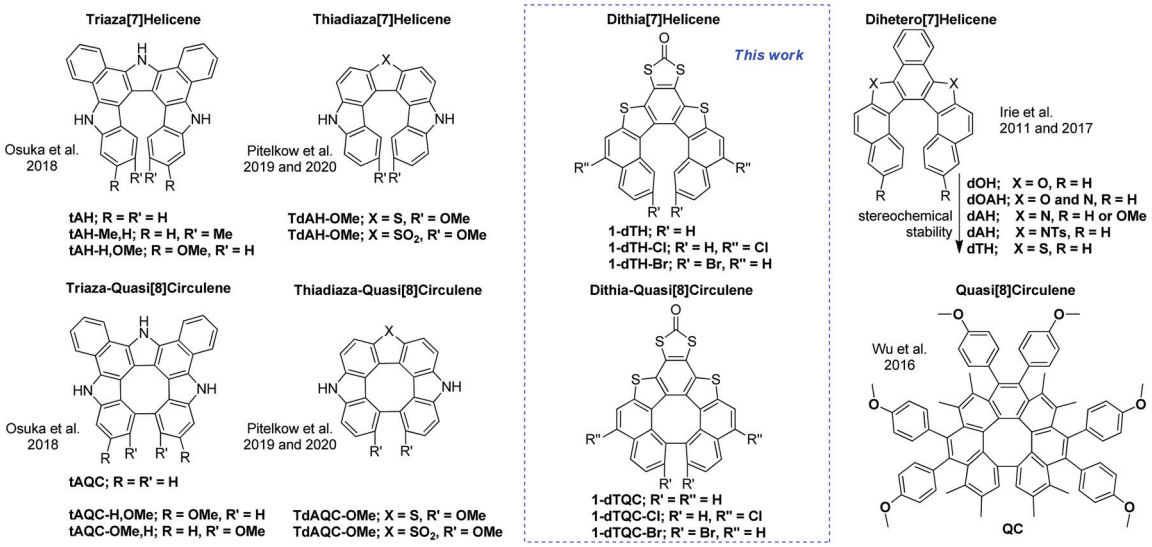

Fig. 1 Examples of Hetero-[7]Helicenes et Quasi[8]Circulenes; those described in this work are highlighted with the blue rectangle.

Accordingly, the methyl substituted all-hydrocarbon quasi[8]circulene (**QC**, Fig. 1, bottom right) has a saddle-like geometry, its [7]helicene moiety being a highly distorted helix. In such compounds the distortion of the geometry of the π-system has been found to be directly responsible of the stereochemical stability. On the other hand, hetero-quasi[8]circulenes, formed of three five-member rings and four phenyls, are less distorted when unsubstituted (**tAQC**s in Fig. 1 and S1,† torsion angles of 26–33°) and racemize at room temperature (calculated enantiomerisation energy of about 6 kcal mol^{-1}),[11] whereas the presence of substituents in the terminal positions (**tAQC** and **TdAQC** with R′ = OMe, Fig. 1 and S1†) highly distorts their geometries and makes possible the separation of the enantiomers (calculated enantiomerisation energy between 38.5 and 42.8 kcal mol^{-1}).[12] Quasi-circulenes are still rare and, in spite of lower stereochemical stability than their helicene counterparts, show peculiar topologies, yet they have never been used in electroactive materials.

In this respect, the introduction of helical chirality in precursors providing chiral conducting and photoactive materials[13] opens new avenues towards the observation of synergistic phenomena involving chirality and conductivity, such as the electrical magnetochiral anisotropy effect (eMChA),[14] or chirality and light emission, such as circularly polarized luminescence (CPL).[4,13] Two of the most valuable families of chiral electroactive precursors are those of tetrathiafulvalenes (TTF)[15,16] and metal dithiolene complexes,[17,18] which we have been recently used in combination with helicene backbones into helicene-TTF[19] and helicene-metal-dithiolene complexes,[20] showing redox switchable chiroptical and CPL properties, respectively. Note that TTF and dithiolene ligands are closely related since they usually have 1,3-dithiol-2-ones as common synthetic precursors,[21–23] therefore the straightforward access to the latter represents a crucial step towards the former.

We report herein the synthesis, crystalline structures and chiroptical properties of unprecedented dithia[7]helicene and dithia-quasi[8]circulenes to which a 1,3-dithiol-2-one unit is fused, together with DFT calculations shedding light on mechanistic issues and supporting the chiroptical properties. As mentioned above, the presence of the dithiolone unit opens ways towards both TTFs and metal-dithiolene complexes, whereas that of the heteroatoms has the benefit to bring chemical versatility, tune the electronic properties and improve intermolecular interactions in the solid state.

2. Results and discussion

2.1. Synthesis and redox properties

The key intermediate bis-naphtho-thiophene-1,3-dithiol-2-one **4** has been obtained following the synthetic route shown in Scheme 1. The starting material 2-bromonaphtho[2,1-*b*]-thiophene **2a** has been obtained in accordance with described procedures[24–26] and easily crystallized to give suitable single crystals for X-ray diffraction (Fig. S2†). The di-naphthothiophene-ethyne **3** has been synthesized in only one step by the cross-coupling of **2** with calcium carbide as acetylene source[27] in the presence of palladium catalyst and a base. The yields of the cross-coupling reactions have been massively improved by using the 2-iodonaphtho[2,1-*b*]-thiophene **2b** instead of **2a**. Further, the 1,3-dithiol-2-one **4**, bearing two naphthothiophene units, was obtained by a radical chain process, adapted from the work of Gareau *et al.*,[28] using **3** and diisopropyl xanthogen disulphide in the presence of azobis(isobutyronitrile) (AIBN). The structure of the 1,3-dithiol-2-one **4** was confirmed by X-ray diffraction analysis on single crystals obtained by evaporation from halogenated solvents (Fig. S3†).

The desired helicene and quasi-circulene molecules have been obtained as racemates by oxidative dehydrocyclisation

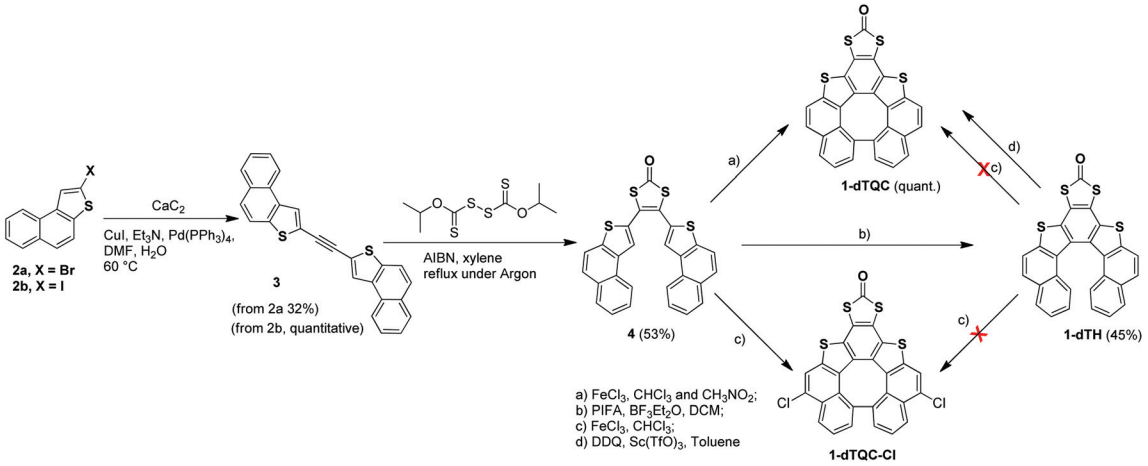

Scheme 1 Synthetic pathways for dithia[7]helicene **1-dTH** and the corresponding dithia-quasi[8]circulenes **1-dTQC** and **1-dTQC-Cl**.

from molecule **4**. The first choice of oxidation agent was $FeCl_3$. Thus, dithia-quasi[8]circulene **1-dTQC-Cl** was quantitatively obtained when up to 10 equivalents of solid $FeCl_3$ were added on top of a chloroform solution of **4** independently of the reaction time (Table 1, entries 1 and 2). Similar electrophilic substitution has been previously reported when solid $FeCl_3$ was used as oxidation reagent for the dehydrocyclisation reaction.[29] If the oxidation agent is added as nitromethane solution, **1-dTQC** is quantitatively obtained after only one hour of reaction (Table 1, entry 3). With only one equivalent of the oxidation agent in a mixture of chloroform and nitromethane, the reaction is not complete but does show the formation of the dithia[7]helicene **1-dTH** together with its corresponding quasi[8]circulene (Table 1, entry 4). Thus, using $FeCl_3$ as oxidation agent one can selectively obtain either the dithia-quasi[8]circulene **1-dTQC** and its chlorinated equivalent **1-dTQC-Cl** but not the dithia[7]helicene **1-dTH**. The latter has been successfully synthesized by intramolecular dehydrocyclisation with the hypervalent iodine(III) reagent phenyliodine bis(trifluoroacetate) (PIFA). In this respect, two sets of conditions have been tried at low temperature (Table 1, entries 5–7). The reaction does not provide the desired product when only PIFA alone is used, instead it has been obtained with activated PIFA-$BF_3{\cdot}Et_2O$ (boron trifluoride diethyl etherate), similarly to previously reported procedures.[30] Selectivity towards the dithia[7]helicene **1-dTH** over the dithia-quasi[8]circulene **1-dTQC** was achieved when controlling the amount of the oxidizing reagent (Table 1, entry 7). With 1.2 equivalents of reagent the reaction is not complete affording **1-dTH** in 45% yield and no formation of **1-dTQC**. Note that, rather surprisingly, complete selectivity towards monoaza-[7]helicene was recently reported by Ema *et al.*[31] when using up to 10 equivalents of $FeCl_3$, whereas the presence of methoxy substituents induced selective formation of the monoaza-quasi[8]circulene in the same reaction conditions. In their work the selectivity towards the quasi-circulene was favoured by higher spin density at the terminal benzene rings of the radical cation form induced by the nature of the substituents. In our case the dithia-quasi[8]circulene **1-dTQC** could not be obtained by sequential oxidative dehydrocyclisation passing through the helicenic form as described for thiadiaza-quasi[8]circulenes **TdAQC** derivatives (Fig. 1), which have been obtained with only one equivalent of oxidizing reagent (chloranil-$BF_3{\cdot}Et_2O$).[12] In fact, dithia[7]helicene **1-dTH** treated with an excess of $FeCl_3$ over long reaction time or with chloranil (tetrachloro-1,4-benzoquinone)-$BF_3{\cdot}Et_2O$ could not be further cyclized to the corresponding quasi[8]circulene (Table S1†). These results suggest that the reaction cannot be done stepwise using $FeCl_3$ or chloranil as oxidants and the formation of quasi-circulene from **4** points towards a mechanism which does not involve a helicene intermediate. We thus hypothesize that if the starting material **4** is oxidized to dication, it undergoes cyclization between the terminal benzene rings followed by a very fast second cyclization between the thiophene units to provide the quasi[8]circu-

Table 1 Oxidative dehydrocyclisation conditions of bis-naphtho-thiophene-1,3-dithiol-2-one **4**

	Oxidant	Eq.	Solvent	Reaction time	Product
1	Solid $FeCl_3$	Excess	$CHCl_3$	60 h (rt)	**1-dTQC-Cl** (quant.)
2	Solid $FeCl_3$	10	$CHCl_3$	3 h (rt)	**1-dTQC-Cl** (quant.)
3	Solution of $FeCl_3/CH_3NO_2$	10	$CHCl_3/CH_3NO_2$	1 h (rt)	**1-dTQC** (quant.)
4	Solution of $FeCl_3/CH_3NO_2$	1	$CHCl_3/CH_3NO_2$	up to 80 h (rt)	**4** + **1-dTQC** + **1-dTH**
5	PIFA	1	CH_2Cl_2	0.5 h (−78 °C), 1 h (rt)	**4**
6	PIFA-$BF_3{\cdot}Et_2O$	Excess	CH_2Cl_2	0.5 h (−78 °C)	**1-dTQC** (quant.)
7	PIFA-$BF_3{\cdot}Et_2O$	1.2	CH_2Cl_2	1 h (−78 °C)	**4** + **1-dTH** (45%)

lene **1-dTQC**. Nonetheless, the dehydrocyclisation of **1-dTH** to afford the corresponding quasi-circulene **1-dTQC** could be performed with DDQ (2,3-dichloro-5,6-dicyano-1,4-benzoquinone), which is a stronger oxidizing reagent (Table S1†).

The electrochemical properties of the precursor and final products have been investigated using cyclic voltammetry (Fig. 2 and S18†). The electron donor character of the precursor and derivatives is rather similar, with oxidation potential values around 1.4 V *vs.* SCE, but only dithia[7]helicene **1-dTH** and quasi[8]circulene **1-dTQC** show reversible redox character. At high scan rates partial reversibility of the oxidized form of **4** is observed whereas the recorded CVs at low scan rates (50 and 100 mV s^{-1}) are irreversible indicating a high reactivity of the radical cation form. On the contrary, the CVs of **1-dTH** at different scan rates are the same suggesting a higher stability of the mono-oxidized form of the helicene compared to **4**. This result is in accordance with our observations on the chemical oxidation of the helicene and the difficulty to form the quasi [8]circulene from the corresponding helicene.

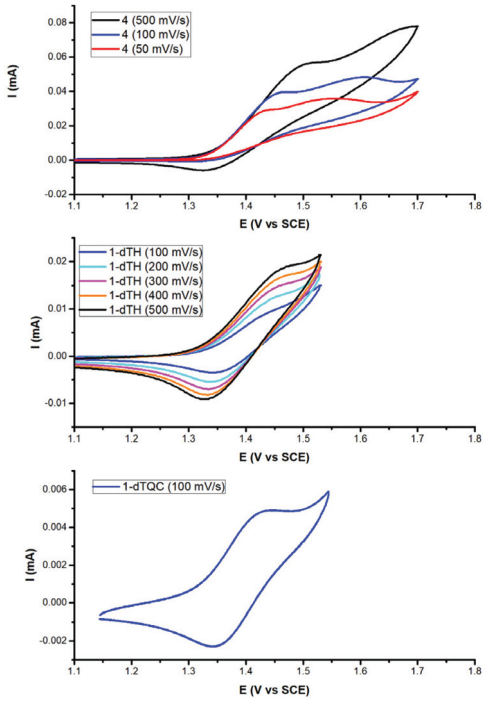

Fig. 2 Cyclic voltammetry of **4** (1.24 mM), **1-dTH** (1.24 mM) and **1-dTQC** (1.04 mM) using $TBAPF_6$ electrolyte (100 mM solution in dichloromethane) at different scan rates.

2.2. Solid state characterization

Single crystals of the racemic forms of dithia[7]helicene **1-dTH** and of quasi[8]circulene **1-dTQC** have been obtained by evaporation from halogenated solvents such as dichloromethane and chloroform (Fig. 3). Poorer crystallographic data have been obtained for **1-dTQC-Cl** therefore it is not included in the discussion, nevertheless the data was suitable to confirm the structure (Fig. S11–S14†).

Dithia[7]helicene **1-dTH** crystallizes in the triclinic system, $P\bar{1}$ space group, with two independent molecules in the unit cell (**A** and **B** of *M* and *P* helicity, respectively). The stacking of the molecules is directed by S···S interaction along the *b* and *a* axes. Within the stack molecules alternate in a *head-to-tail* fashion, with a small overlap taking place only between the S rich parts of the molecules (donor part) and with a lateral shift with respect to each other of 1.470 Å and 1.641 Å for **A** and **B**, respectively (Fig. S4†). The result of this arrangement gives a segregation of the 1,3-dithiol-2-one unit and the carbon based helicene side within the packing (Fig. S5 and S6†). The small

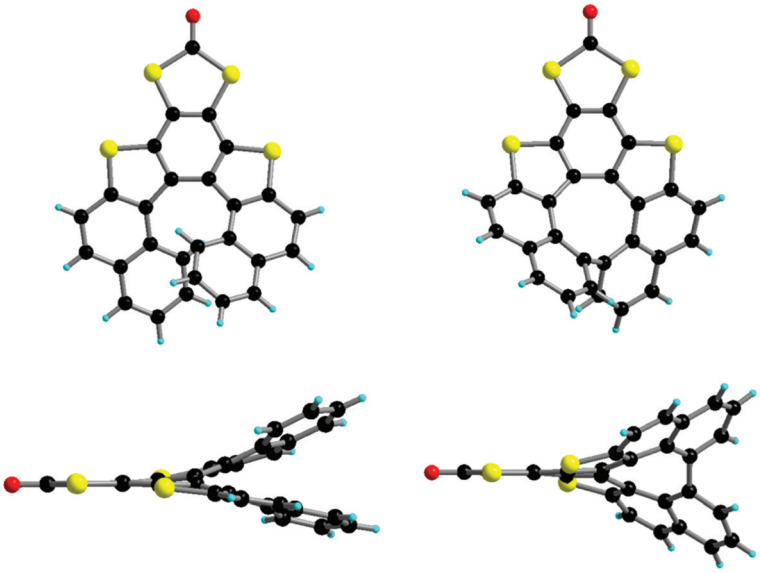

Fig. 3 Top and side view of dithia[7]helicene **1-dTH** (*M*) (left), dithia-quasi[8]circulenes **1-dTQC** (*P*) (right) in the crystal structures of the racemic forms of the two compounds.

overlap is due to steric crowdedness of the helicene rings and is being directed by intermolecular interactions between the S atoms of both types (thiophene and dithiolene). In the *bc* plane all S atoms interact laterally by $S_{th}\cdots S_{dithiolene}$ short contacts of 3.390–3.579 Å resulting in the formation of infinite layers of alternate –**A**–**B**–molecules (Fig. 4). Other notable small distances between the stacks of **A** and stacks of **B** consist in C–H···π inter-stack interactions of the helicene parts of the molecules (Fig. S7†). In the stack, along the *a* axis, these layers show $S_{dithiolene}\cdots S_{dithiolene}$ distances of 3.773, 4.045 Å and $S_{th}\cdots S_{dithiolene}$ of 3.940, 4.079 Å between the type **A** molecules and, respectively, of 4.009, 4.015 Å and of 3.857, 4.038 Å between the type **B** molecules (Fig. 5).

Racemic quasi[8]circulene **1-dTQC** crystallizes in the monoclinic system, $P2_1/c$ space group, with the asymmetric unit formed by one independent molecule. In the stack **1-dTQC** molecules are disposed in a *head-to-tail* manner along *a* and interact along *c* through $S_{dithiolene}\cdots S_{dithiolene}$ (green) contacts (Fig. S8–S10†). Molecules of alternating layers are tilted with respect to each other of about 48.8° and stack *via* short lateral interactions $S_{th}\cdots S_{dithiolene}$ (grey) and $S_{dithiolene}\cdots S_{dithiolene}$ (green) of about 3.409, 3.492 and 3.392 Å, respectively (Fig. 6).

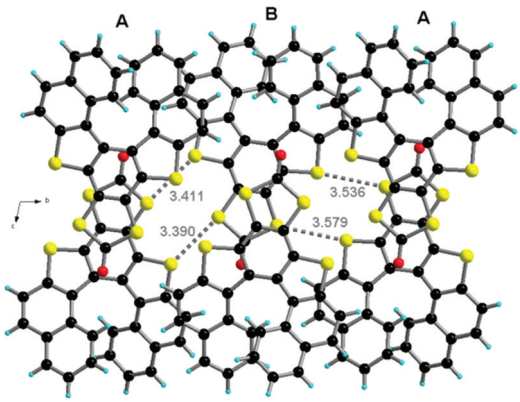

Fig. 4 Intermolecular lateral interactions between molecules A and B, $S_{th}\cdots S_{dithiolene}$ (grey) in the structure of dithia[7]helicene **1-dTH**.

In helicenes and quasi-circulenes the values of the internal torsion angles of each of the constituting rings (**A** to **D** for [7] helicenes and quasi[8]circulenes) and their sums are a good indicator of the degree of helical twist (Table 2). Equivalent helicenes with a ring of five atoms instead of the phenyl ring **A** have a smaller sum of the internal torsion angles (between 56.9 to 61.9°) than the sum in the dithia[7]helicene **1-dTH** (*ca.* 76°) thus suggesting a more important helical twist and a higher stability of the stereoisomers of the latter.[32] In dithia[7] helicene **1-dTH** the twist is high around **A**, **B** and **B′** rings whereas in quasi[8]circulene **1-dTQC** it is less important around rings **B** and **B′**. Quasi[8]circulene shows significant distortion of planarity of rings **A**, **C** and **C′** and high inter-planar angle of the **D** and **D′** rings of *ca.* 61° and 64° (*ca.* 35° for **1-dTH**) suggesting a high degree of helical twist imposed by the **D–D′** covalent bond. All-hydrocarbon quasi[8]circulene (**QC**, Fig. 1), in which the **B** and **B′** rings are phenyls, present similar characteristics with smaller torsions angles of these rings and high angle of *ca.* 79° between the planes of rings **D** and **D′**.[8] Moreover, the degree of torsion of the helicenic unit of quasi-circulenes described in here, seen only through the twist around ring **A**, is comparable to previously reported double dioxa[7]helicene (values between 28.6° and 31.8°)[33] which is about 10° superior to **1-dTH** (*ca.* 18°, Fig. S15, ESI†).

2.3. Mechanistic issues

Density functional theory (DFT) calculations have been performed in order to rationalize the formation of the quasi[8]circulene **1-dTQC** *via* a cationic reaction mechanism (the computational methodology is detailed in the ESI†). Thus, the precursor **4** and dithia[7]helicene **1-dTH** have been optimized as neutral species, radical cations (**4-cat** and **1-dTH-cat**), dihydro-radical cations (**4′-cat** and **1-dTH′-cat**), dications (**4-dicat** and **1-dTH-dicat**), dihydro-dications (**4′-dicat** and **1-dTH′-dicat**), and tetrahydro-dications (**4″-dicat**) forms. The different dications have been considered in their singlet state since, for example, the optimization of **4-dicat** as both singlet and triplet states indicates that the latter is higher in energy by 7.17 kcal mol^{-1} than the former. The higher stability of the singlet state of the dications is not surprising when considering the extent of the

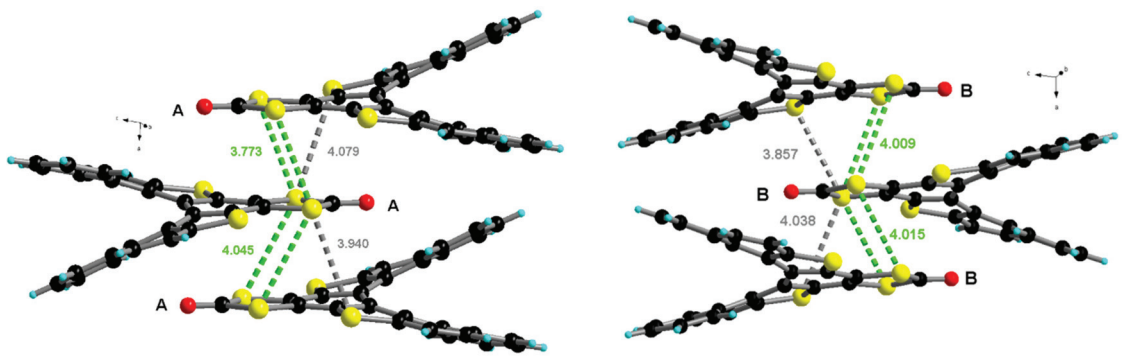

Fig. 5 View along the *a* axis of the intermolecular interactions (Å) between molecules of type A and molecules of type B, $S_{th}\cdots S_{dithiolene}$ (grey) and $S_{dithiolene}\cdots S_{dithiolene}$ (green) in the structure of dithia[7]helicene **1-dTH**.

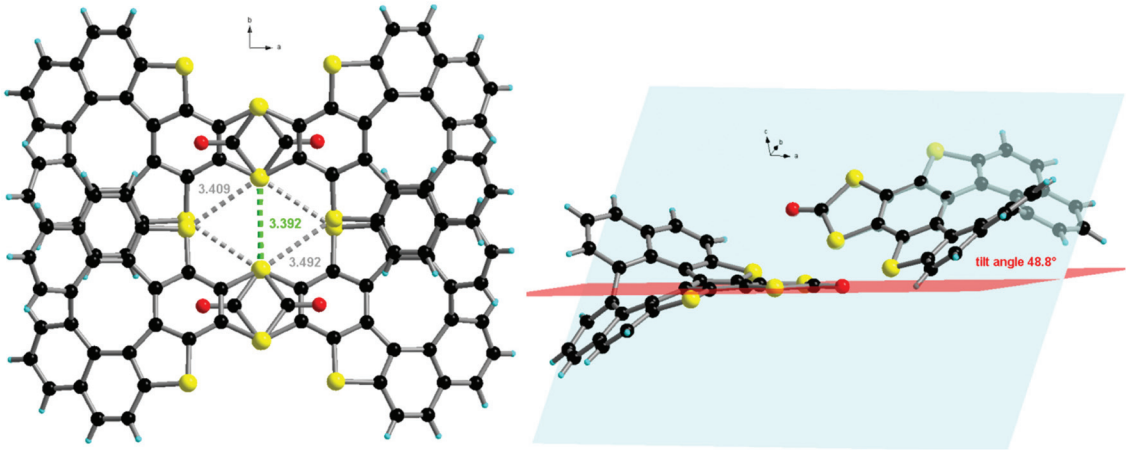

Fig. 6 Tilt angle (°) and intermolecular lateral interactions (Å) between molecule of alternating layers together with $S_{th}\cdots S_{dithiolene}$ (grey) and $S_{dithiolene}\cdots S_{dithiolene}$ (green) in the structure of quasi[8]circulene **1-dTQC**.

Table 2 Values of the torsion angles (°) for each of the constituting rings, together with the dihedral angle (°) of the terminal rings in dithia[7]helicene **1-dTH**, quasi[8]circulenes **1-dTQC**, and in all-hydrocarbon quasi[8]circulene **QC**[8]

	Torsion angles (°)			
	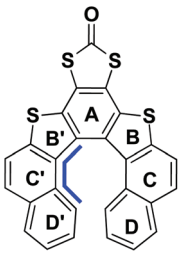		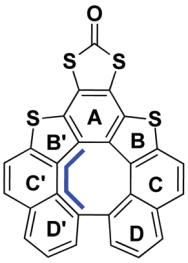	
Ring	**1-dTH**		**1-dTQC**	**QC** (Fig. 1)
A	18.23	18.19	32.47	63.9
B	17.42	20.68	1.13	3.1
B′	18.65	15.41	9.25	6.2
C	10.61	12.17	25.61	48
C′	11.42	10.41	32.49	47.3
Total (average)	76.33 (15.26)	76.86 (15.37)	101.95 (20.39)	168.5 (33.7)
D			29.42	16.3
D′			27.61	23.5
D–D′			81.40	91.7
	Helical curvature[a] (°)			
D–D′	35.77	35.00	61.17	79.2

[a] Interplanar angle (angle between the planes of the terminal cycles).

conjugation between the two naphthothiophene moieties illustrated by the shape of the HOMO of **4-dicat** (Fig. 7). The SOMO topology of **4-cat** suggests the formation of helicene *via* the **4′-cat-cis** intermediary through a disrotatory ring closure (Fig. 7, top). A dication route is not plausible for the access to helicene as suggested by the absence of electronic density in the HOMO of **4-dicat** on the carbon atoms of the thiophene rings involved in the ring closure. On the contrary, the electron density distribution in the HOMO of **4-dicat** points towards a favourable formation of the first C–C bond between the terminal phenyl rings that would provide the dihydro-intermediate **4′-circ-dicat**, which does not converge upon geometry optimization but leads to a second C–C bond formation between the thiophene rings to give the tetrahydro-intermediate **4″-dicat**. Then, dehydrogenation takes place to afford the desired quasi[8]circulene **1-dTQC** (Fig. 7, middle). Furthermore, the possibility to obtain the circulene from the helicene *via* a radical cation intermediate has been considered. The SOMO topology of **1-dTH-cat** (Fig. S19†) clearly shows that the thermal ring closure towards **1-dTH′-cat** is not favourable, thus excluding the formation of quasi[8]circulene **1-dTQC** from the radical cation of the helicene *via* the dihydro-radical cation form. Moreover, the **1-dTH-dicat** seems to be the proper intermediate for the formation of the quasi[8]circulene from **1-dTH**, which, although is not converging, leads directly to **1-dTH′-dicat** (Fig. 7, bottom). These results allow us to hypothesize that under our experimental conditions dithia[7]helicene **1-dTH** could be formed from **4** *via* the radical cation route only, whereas quasi[8]circulene **1-dTQC** could be produced from both **4** and **1-dTH** *via* the dication route. Moreover, the electronic density of the HOMO of **1-dTQC** (Table S7†) explains the selectivity of the double electrophilic substitution of chlorine on the outer positions to afford de **1-dTQC-Cl** circulene.

2.4. Enantiomerisation energy barriers and enantiomer resolution

The enantiomerisation barriers for **1-dTH** and **1-dTQC** were estimated by DFT calculations and experimentally determined by first-order kinetics measurements (details in the ESI†). As seen in Fig. 8 the calculated energy barrier is higher for the helicene than the corresponding quasi-circulene. The isomerization barriers of dithia[7]helicenes have been estimated at 36.8 and 36.9 kcal mol^{-1} for **1-dTH-Cl** and **1-dTH**, respectively. These values are in perfect agreement with the experimentally determined one at 37.0 kcal mol^{-1} for **1-dTH**. **1-dTH-Cl** and **1-**

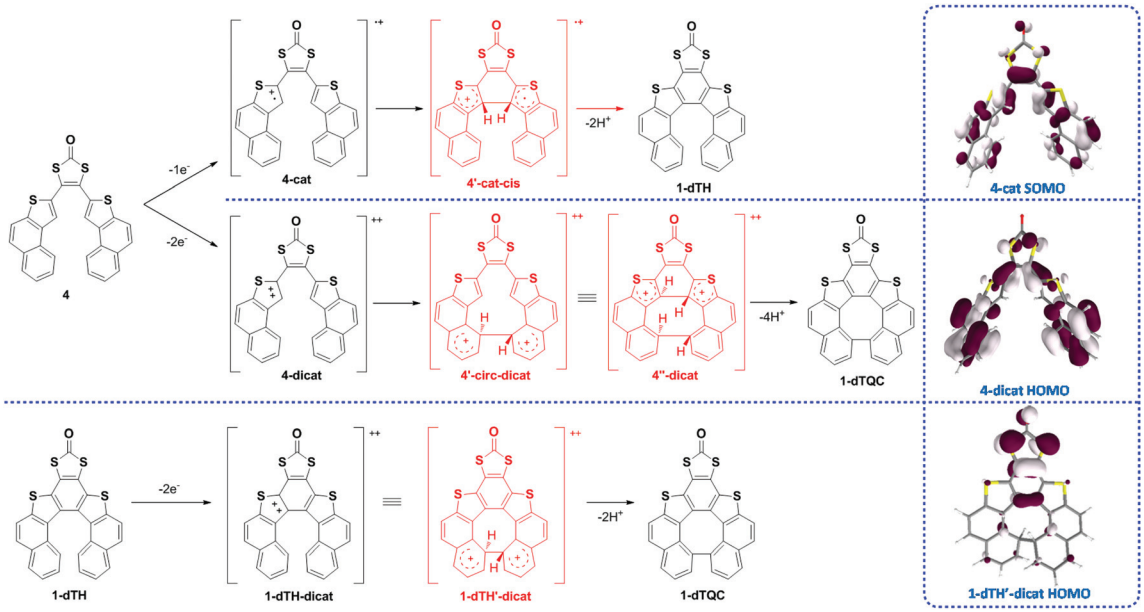

Fig. 7 Proposed reaction mechanism for helicene **1-dTH** and quasi-circulene **1-dTQC**, together with the optimized orbitals for the radical cation and dication of **4** and dihydro-dication of **1-dTH**. In red are highlighted the cyclized dihydro- and tetrahydro-radical cation and dication intermediates.

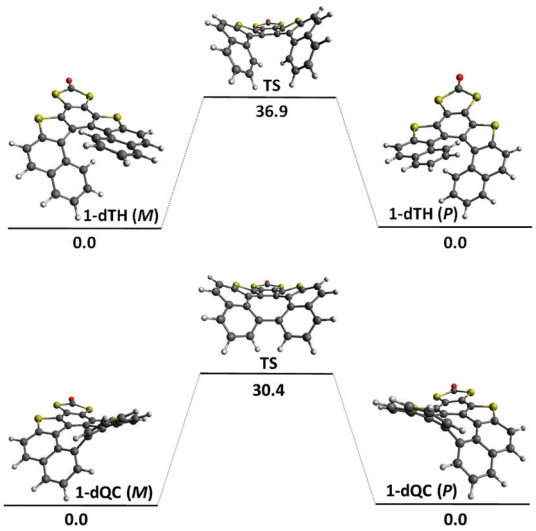

Fig. 8 Isomerisation process from *M* to *P* enantiomer together with the calculated relative Gibbs free energy (kcal mol^{-1}) for **1-dTH** (left) and **1-dTQC** (right) (the computational methodology is detailed in the ESI†).

dTH-Br (Fig. 1) have been included in the theoretical study for comparison purposes. As expected, a substituent in the external position of the helix does not induce any effect on the barrier, whereas if inserted at the two extremities of the helix the impact is highly significant (Table 3, calculated enantiomerisation barriers for both dithia[7]helicene and dithia-quasi [8]circulenes with Cl external substituent and Br at the extremities of the helix). The enantiomerisation energy estimated by DFT calculations indicates for **1-dTH** the highest barrier within the unsubstituted dihetero[7]helicene series with O, ON, N and S heteroatoms. In the case of diaza[7]helicene **dAH** substitution on the N atoms induces a slightly higher barrier which still remains inferior to dithia[7]helicene, whereas substituents on the two extremities of the helix have, as expected, greater influence (Fig. 1, Table 3 and Table S4†).[34] The stereochemical stability of unsubstituted **1-dTH** is the highest amongst simple dihetero- and trihetero-[7]helicenes reported to date at the exception of π-extended double dioxa[7]helicene and triple dioxa[7]helicene which attain values of 50.5 kcal mol^{-1},[33] 51.9 and 77.4 kcal mol^{-1},[35] respectively. In the trihetero[7]helicene series replacing one N with S and the methyl substituent with methoxy induces an increase of the barrier up to 32.9 kcal mol^{-1} for **TdAH-OMe,H**[12] *vs.* **tAH-Me,H**[11] (25.5 kcal mol^{-1}). Similar to helicenes, twisted C_s-symmetry of the transition state has been predicted for dithia-quasi[8]circulene **1-dTQC** and the calculated enantiomerisation energy is of 30.4 kcal mol^{-1}, suggesting a lower stereostability than the **1-dTH** but still high enough to allow the separation of the enantiomers. The experimentally determined value for **1-dTQC** of 29.8 kcal mol^{-1} is in perfect agreement with the calculations. Thus, the dithia-quasi[8]circulenes reported in this work have the highest stereostability amongst reported unsubstituted quasi-circulenes.

Enantiomers of both **1-dTH** and **1-dTQC** have been separated by chiral HPLC with chiral stationary phases (Chiralpak IE and (*S*,*S*)-Whelk-O1) and mixtures of hexane/dichloromethane as mobile phases (ESI for details†). As predicted by the theory and confirmed experimentally, the enantiomerisation energies are high enough to allow separation of the enantiomers which show mirror image circular dichroism (CD)

Table 3 Estimated and experimentally (in brackets) determined enantiomerisation energies of [7]helicene and their corresponding quasi[8]circulenes (in green – synthesized molecules, in grey – calculated molecules for comparison)

	[7]Helicenes		Quasi[8]Circulenes		Ref.
Enantiomerisation energy DFT (exp) (kcal mol^{-1})	**1-dTH**	36.9 (37.0)	**1-dTQC**	30.4 (29.8)	This work
	1-dTH-Cl[a]	36.8	**1-dTQC-Cl**[a]	31.6	
	1-dTH-Br[b]	43.3	**1-dTQC-Br**[b]	69.3	
	dTH(S)	35.4, 36.5[c]	**dTQC(S)**[c]	30.4[c]	34
	tAH	23	**tAQC**	6	11
	tAH-Me,H	25.5 (23.8)	—		
	tAH-H,OMe	22.8	**tAQC-H,OMe**	5.2	
	—		**tAQC-OMe,H**	42.8	36
	TdAH-OMe,H (S)	32.9	**TdAQC-OMe,H (S)**	38.5	12
	TdAH-OMe,H (SO2)	31.9	**TdAQC-OMe,H (SO2)**	38.4	
	[7]carbo-helicene	(41.7)	**QC**	35.9	8 and 37

[a] Substituent Cl is situated at the exterior of the helix (see Fig. 1). [b] Substituent Br at the extremities of the helix (see Fig. 1). [c] Not reported previously, values calculated by DFT in this work for comparison reason.

spectra (Fig. 9). The absolute configuration of the enantiomers was deduced by comparison with the calculated CD spectra. For both **1-dTH** and **1-dTQC** the first eluted fraction corresponds to *M* and the second one to *P* enantiomers (black and red curves respectively) and the relation between the absolute configuration and the optical rotation follows the general trend observed in helicenes. Thus, *M* enantiomers are levorotatory for both **1-dTH** and **1-dTQC**, with specific optical rotation values of −1050 and −700 deg mL g^{-1} dm^{-1} ($[\alpha]_D^{25}$ in CH_2Cl_2) (Tables S5 and S6†). In both cases, the first eluted fraction shows a first negative Cotton effect at low energy, 407 nm for **1-dTH** and 405 nm for **1-dTQC**, in contrast to what was observed when comparing other [7]helicene and quasi-[8]circulenes **tAH-Me,H** and **tAQC-OMe,H**. In that particular case the helicene showed a positive Cotton effect at low energy whereas the circulene was negative for the same enantiomer.[11,36] Moreover, in our case the CD intensities of **1-dTH** and **1-dTQC** are comparable whereas azahepta[8]circulene recently reported[31] present much weaker Cotton effects than their helicenic equivalents.

Thus, the first two low energy bands, arising at 407/393 nm (**1-dTH**) and 405/383 nm (**1-dTQC**) and calculated at 399/370 nm (**1-dTH**) and 394/357 nm (**1-dTQC**), correspond to almost pure HOMO→LUMO and HOMO−1→LUMO transitions (Tables S8 and S9†). In the high energy area, the stronger Cotton effects predicted by theory correspond, for example, to excitations at 273 nm (experimental at 279 nm) for **1-dTH** and 294 nm (experimental at 296 nm) for **1-dTQC**, which are described predominantly by HOMO→LUMO+6 and HOMO→LUMO+4 transitions, respectively (Tables S8 and S9†). Whereas for helicene the predicted spectra are reproducing the experimental ones in terms of rotational strength, for circulene the stronger experimental CD signal at 252 nm would be predominantly a HOMO−4→LUMO+1 transition, calculated as well at 252 nm, but less intense. Note the non-negligible involvement of the dithiolene ring in all these CD active transitions, according to the participation of the dithiolene atoms to the corresponding molecular orbitals, witnessing its conjugation with the helical backbone.

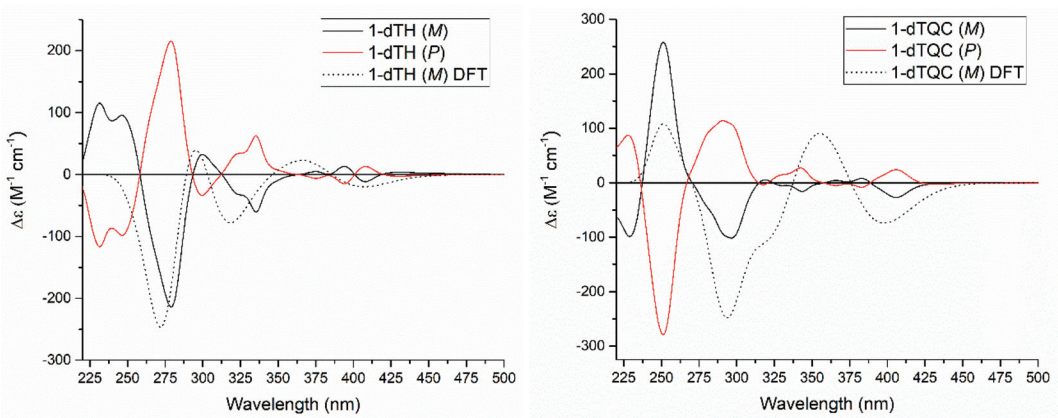

Fig. 9 CD spectra (black first and red second eluted fractions) of **1-dTH** and **1-dTQC** 0.19 mM in dichloromethane, together with the DFT calculated CD spectra of the *M* enantiomers (dotted black).

3. Conclusions

Within this work, unprecedented dithia[7]helicene and dithia-quasi[8]circulenes decorated with 1,3-dithio-2-one have been synthesized through an elegant method involving a one step simple and double oxidative dehydrocyclisation of a bis-naphtho-thiophene-1,3-dithiol-2-one precursor. A selectivity towards quasi[8]circulene has been observed with $FeCl_3$ oxidant whereas the helicene has been preferentially obtained at low temperature with PIFA-BF_3·Et_2O oxidant. DFT calculations suggest a mechanism through a radical cation intermediate for the synthesis of dithia[7]helicene and dication in the case of dithia-quasi[8]circulene. Theoretical simulations estimate enantiomerisation barriers of 36.9 kcal mol^{-1} for **1-dTH** and 30.4 kcal mol^{-1} for **1-dQC** in excellent agreement with the experimentally determined values of 37.0 and 29.8 kcal mol^{-1}, respectively. Thus, dithia[7]helicene and dithia-quasi[8]circulene have the highest stereostability amongst simple dihetero- and trihetero-[7]helicenes and unsubstituted quasi-circulenes, respectively. Enantiomers of both helicene and quasi-circulenes show stereostability at room temperature and have been successfully separated by chiral chromatography. Importantly, the 1,3-dithio-2-one motif should further give straightforward access to TTF and metal-dithiolene complexes, fused in the middle of the helical unit, which are valuable precursors for conducting materials with helical chirality.

References

1 Y. Shen and C.-F. Chen, Helicenes: Synthesis and Applications, *Chem. Rev.*, 2012, **112**, 1463–1535.

2 M. Gingras, One hundred years of helicene chemistry. Part 3: applications and properties of carbohelicenes, *Chem. Soc. Rev.*, 2013, **42**, 1051–1095.

3 Y. Yang, R. C. da Costa, M. J. Fuchter and A. J. Campbell, Circularly polarized light detection by a chiral organic semiconductor transistor, *Nat. Photonics*, 2013, **7**, 634–638.

4 K. Dhaibi, L. Favereau and J. Crassous, Enantioenriched Helicenes and Helicenoids Containing Main-Group Elements (B, Si, N, P), *Chem. Rev.*, 2019, **119**, 8846–8953.

5 J. H. Dopper, D. Oudman and H. Wynberg, Dehydrogenation of heterohelicenes by a Scholl type reaction. Dehydrohelicenes, *J. Org. Chem.*, 1975, **40**, 3398–3401.

6 K. Kawasumi, Q. Zhang, Y. Segawa, L. T. Scott and K. Itami, A grossly warped nanographene and the consequences of multiple odd-membered-ring defects, *Nat. Chem.*, 2013, **5**, 739–744.

7 Z. Qiu, S. Asako, Y. Hu, C.-W. Ju, T. Liu, L. Rondin, D. Schollmeyer, J.-S. Lauret, K. Mullen and A. Narita, Negatively Curved Nanographene with Heptagonal and [5] Helicene Units, *J. Am. Chem. Soc.*, 2020, **142**, 14814–14819.

8 C.-N. Feng, W.-C. Hsu, J.-Y. Li, M.-Y. Kuo and Y.-T. Wu, Per-Substituted [8]Circulene and Its Non-Planar Fragments: Synthesis, Structural Analysis, and Properties, *Chem. – Eur. J.*, 2016, **22**, 9198–9208.

9 (*a*) M. Rickhaus, M. Mayor and M. Juricek, Strain-induced helical chirality in polyaromatic systems, *Chem. Soc. Rev.*, 2016, **45**, 1542–1556; (*b*) M. Rickhaus, M. Mayor and M. Juricek, Chirality in curved polyaromatic systems, *Chem. Soc. Rev.*, 2017, **46**, 1643–1660.

10 A. Rajca, M. Miyasaka, S. Xiao, R. J. Boratybski, M. Pink and S. Rajca, Intramolecular Cyclization of Thiophene-Based [7]Helicenes to Quasi-[8]Circulenes, *J. Org. Chem.*, 2009, **74**, 9105–9111.

11 F. Chen, T. Tanaka, T. Mori and A. Osuka, Synthesis, Structures, and Optical Properties of Azahelicene Derivatives and Unexpected Formation of Azahepta[8]circu-lenes, *Chem. – Eur. J.*, 2018, **24**, 7489–7497.

12 B. Lousen, S. K. Pedersen, P. Bols, K. H. Hansen, M. K. Pedersen, O. Hammerich, S. Bondarchuk, B. Minaev, G. V. Baryshnikov, H. Ågren and M. Pittelkow, Compressing a Non-Planar Aromatic Heterocyclic [7]Helicene to a Planar Hetero[8]Circulene, *Chem. – Eur. J.*, 2020, **26**, 4935–4940.

13 F. Pop, N. Zigon and N. Avarvari, Main-Group-Based Electro- and Photoactive Chiral Materials, *Chem. Rev.*, 2019, **119**, 8435–8478.

14 F. Pop, P. Auban-Senzier, E. Canadell, G. L. J. A. Rikken and N. Avarvari, Electrical magnetochiral anisotropy in a bulk chiral molecular conductor, *Nat. Commun.*, 2014, **5**, 3757.

15 N. Avarvari and J. D. Wallis, Strategies towards chiral molecular conductors, *J. Mater. Chem.*, 2009, **19**, 4061–4076.

16 N. Mroweh, C. Mézière, F. Pop, P. Auban-Senzier, P. Alemany, E. Canadell and N. Avarvari, In Search of Chiral Molecular Superconductors: κ-[(*S*,*S*)-DM-BEDT-TTF]$_2$$ClO_4$ Revisited, *Adv. Mater.*, 2020, **32**, 2002811.

17 F. Pop and N. Avarvari, Chiral metal-dithiolene complexes, *Coord. Chem. Rev.*, 2017, **346**, 20–31.
18 D. G. Branzea, F. Pop, P. Auban-Senzier, R. Clérac, P. Alemany, E. Canadell and N. Avarvari, Localization versus Delocalization in Chiral Single Component Conductors of Gold Bis(dithiolene) Complexes, *J. Am. Chem. Soc.*, 2016, **138**, 6838–6851.
19 T. Biet, A. Fihey, T. Cauchy, N. Vanthuyne, C. Roussel, J. Crassous and N. Avarvari, Ethylenedithio-Tetrathiafulvalene-Helicenes: Electroactive Helical Precursors with Switchable Chiroptical Properties, *Chem. – Eur. J.*, 2013, **19**, 13160–13167.
20 T. Biet, T. Cauchy, Q. Sun, J. Ding, A. Hauser, P. Oulevey, T. Burgi, D. Jacquemin, N. Vanthuyne, J. Crassous and N. Avarvari, Triplet state CPL active helicene–dithiolene platinum bipyridine complexes, *Chem. Commun.*, 2017, **53**, 9210–9213.
21 J. Yamada, H. Akutsu, H. Nishikawa and K. Kikuchi, New Trends in the Synthesis of π-Electron Donors for Molecular Conductors and Superconductors, *Chem. Rev.*, 2004, **104**, 5057–5083.
22 C. Rovira, Bis(ethylenethio)tetrathiafulvalene (BET-TTF) and Related Dissymmetrical Electron Donors: From the Molecule to Functional Molecular Materials and Devices (OFETs), *Chem. Rev.*, 2004, **104**, 5289–5317.
23 R. Kato, Conducting Metal Dithiolene Complexes: Structural and Electronic Properties, *Chem. Rev.*, 2004, **104**, 5319–5346.
24 B. Rungtaweevoranit, A. Butsuri, K. Wongma, K. Sadorn, K. Neranon, C. Nerungsi and T. Thongpanchang, A facile two-step synthesis of thiophene end-capped aromatic systems, *Tetrahedron Lett.*, 2012, **53**, 1816–1818.
25 K. Krajewski, Y. Zhang, D. Parrish, J. Deschamps, P. P. Rollera and V. K. Pathak, New HIV-1 reverse transcriptase inhibitors based on a tricyclic benzothiophene scaffold: Synthesis, resolution, and inhibitory activity, *Bioorg. Med. Chem. Lett.*, 2006, **16**, 3034–3038.
26 K. Clarke, G. Rawson and R. M. Scrowston, Substitiution reaction of naphtho[2,1-*b*]thiophen, *J. Chem. Soc. C*, 1969, **4**, 537–540.
27 (*a*) W. Zhang, H. Wu, Z. Liu, P. Zhong, L. Zhang, X. Huang and J. Cheng, The use of calcium carbide in one-pot synthesis of symmetric diaryl ethynes, *Chem. Commun.*, 2006, 4826–4828; (*b*) R. Saha, D. Arunprasath and G. Sekar, Surface enriched palladium on palladium-copper bimetallic nanoparticles as catalyst for polycyclic triazoles synthesis, *J. Catal.*, 2019, **377**, 673–683.
28 Y. Gareau and A. Beauchemin, Simple Method for the Preparation of 1,3-Dithiol-2-one and 1,3-Dithiol-2-thione, *Phosphorus, Sulfur Silicon*, 1997, **120–121**, 393–394.
29 J. L. Ferguson, M. A. Squire and C. M. Fitchett, Photochemical and oxidative cyclisation of tetraphenylpyrroles, *Org. Biomol. Chem.*, 2017, **15**, 9239–6296.
30 Y. Kita, M. Gyoten, M. Ohtsubo, H. Tohma and T. Takada, Non-phenolic oxidative coupling of phenol ether derivatives using phenyliodine(III) bis(trifluoroacetate), *Chem. Commun.*, 1996, 1481–1482.
31 C. Maeda, S. Nomoto, K. Akiyama, T. Tanaka and T. Ema, Facile Synthesis of Azahelicenes and Diaza[8]circulenes through the Intramolecular Scholl Reaction, *Chem. – Eur. J.*, 2021, **27**, 15699–15705.
32 K. Uematsu, K. Noguchi and K. Nakano, Synthesis and properties of [7]helicene and [7]helicene-like compounds with a cyclopenta[1,2-*b*:4,3-*b*′]dithiophene or dithieno[2,3-*b*:3′,2′-*d*]heterole skeleton, *Phys. Chem. Chem. Phys.*, 2018, **20**, 3286–3295.
33 H. Chang, H. Liu, E. Dimietrieva, Q. Chen, J. Ma, P. He, P. Liu, A. A. Popov, X.-Y. Cao, X.-Y. Wang, Y. Zou, A. Narita, K. Mullen, H. Peng and Y. Hu, Furan-containing double tetraoxa[7]helicene and its radical cation, *Chem. Commun.*, 2020, **56**, 15181–15184.
34 (*a*) R. Irie, A. Tanoue, S. Urakawa, T. Imahori, K. Igawa, T. Matsumoto, K. Tomooka, S. Kikuta, T. Uchida and T. Katsuki, Synthesis and Stereochemical Behavior of a New Chiral Oxa[7]heterohelicene, *Chem. Lett.*, 2011, **40**, 1343–1345; (*b*) Y. Kitahara and K. Tanaka, Synthesis, crystal structure and properties of thiaheterohelicenes containing phenolic hydroxy functions, *Chem. Commun.*, 2002, 932–933; (*c*) M. B. Groen, H. Schadenberg and H. Wynberg, Synthesis and resolution of some heterohelicenes, *J. Org. Chem.*, 1971, **36**, 2797–2809; (*d*) M. B. Groen and H. Wynberg, Optical properties of some heterohelicenes. Absolute configuration, *J. Am. Chem. Soc.*, 1971, **93**, 2968–2974; (*e*) S. Arae, T. Mori, T. Kawatsu, D. Ueda, Y. Shigeta, N. Hamamoto, H. Fujimoto, M. Sumimoto, T. Imahori, K. Igawa, K. Tomooka, T. Punniyamurthy and R. Irie, Synthesis and Stereochemical Properties of Chiral Hetero [7]helicenes Structured by a Benzodiheterole Ring Core, *Chem. Lett.*, 2017, **46**, 1214–1216.
35 F. Zhou, Z. Huang, R. Cheng, Y. Yang and J. You, Triple Oxa[7]helicene with Circularly Polarized Luminescence: Enhancing the Dissymmetry Factors via Helicene Subunit Multiplication, *Org. Lett.*, 2021, **23**, 4559–4563.
36 Y. Matsuo, F. Chen, K. Kise, T. Tanaka and A. Osuka, Facile synthesis of fluorescent hetero[8]circulene analogues with tunable solubilities and optical properties, *Chem. Sci.*, 2019, **10**, 11006–11012.
37 R. H. Martin and M. J. Marchant, Thermal racemisation of hepta-, octa-, and nonahelicene : Kinetic results, reaction path and experimental proofs that the racemisation of hexa- and heptahelicene does not involve an intramolecular double diels-alder reaction, *Tetrahedron*, 1974, **30**, 347–349.